

Efficient Continuous Manifold Learning for Time Series Modeling

Seungwoo Jeong,¹ Wonjun Ko,² Ahmad Wisnu Mulyadi,² Heung-II Suk^{1,2}

¹Department of Artificial Intelligence, Korea University

²Department of Brain and Cognitive Engineering, Korea University

{sw.jeong, wjko, wisnumulyadi, hisuk}@korea.ac.kr

Abstract

Modeling non-Euclidean data is drawing attention along with the unprecedented successes of deep neural networks in diverse fields. In particular, symmetric positive definite (SPD) matrix is being actively studied in computer vision, signal processing, and medical image analysis, thanks to its ability to learn appropriate statistical representations. However, due to its strong constraints, it remains challenging for optimization problems or inefficient computation costs, especially, within a deep learning framework. In this paper, we propose to exploit a diffeomorphism mapping between Riemannian manifolds and a Cholesky space, by which it becomes feasible not only to efficiently solve optimization problems but also to reduce computation costs greatly. Further, in order for dynamics modeling in time series data, we devise a continuous manifold learning method by integrating a manifold ordinary differential equation and a gated recurrent neural network in a systematic manner. It is noteworthy that because of the nice parameterization of matrices in a Cholesky space, it is straightforward to train our proposed network with Riemannian geometric metrics equipped. We demonstrate through experiments that the proposed model can be efficiently and reliably trained as well as outperform existing manifold methods and state-of-the-art methods in two classification tasks: action recognition and sleep staging classification.

1 Introduction

Recently, deep learning has been exhaustively employed as de facto standards for many applications in computer vision, natural language processing, signal processing, and so on by achieving unprecedented successes. However, deep learning has still been relatively underexplored in non-Euclidean data (*e.g.*, graphs or special matrices) representation (Bronstein et al. 2017). Such data are often used for analysis in a variety of areas, including but not limited to: shapes (Chang et al. 2015); graphs and trees (Scarselli et al. 2008; Kipf and Welling 2016); symmetric positive matrices (Moakher 2005; Jayasumana et al. 2013); rotation matrices (Kendall and Cipolla 2017).

Particularly, there is a lack of extension to manifold-valued sequential data. Meanwhile, existing deep learning methodologies, *e.g.*, convolutional neural network (CNN)-based models (Zhen et al. 2019; Chakraborty et al. 2020) or recurrent neural network (RNN)-based models (Chakraborty

et al. 2018), were proposed to deal with the manifold-valued sequential data, suggesting a recursive method for the weighted Fréchet mean to avoid the problems of high computational cost and instability in optimization.

In the meantime, researchers have been focusing on modeling dynamic patterns in continuous time points. For example, neural ordinary differential equation (ODE) (Chen et al. 2018) and its variants (Rubanova, Chen, and Duvenaud 2019; Brouwer et al. 2019) have demonstrated their capability for signals representation by capturing dynamics over the internal hidden states. Similar to neural ODE, manifold ODE (Lou et al. 2020) has also been proposed to learn the dynamics of the states in the Riemannian manifold, aiming to estimate complicated distributions in the framework of normalizing flow (Rezende and Mohamed 2015).

In this work, we propose a novel method of continuous manifold learning on sequential manifold-valued data for time series modeling. Specifically, based on the rigorous mathematical justifications, we propose to exploit a diffeomorphism mapping between Riemannian manifolds and a Cholesky space (Lin 2019), by which it becomes feasible to efficiently solve optimization problems and to reduce computational costs greatly. We define and estimate a diffeomorphism between symmetric positive definite (SPD) manifolds and Cholesky manifolds. We solve an optimization problem under the SPD constraints and achieve an effective computation cost by re-defining complex operations. Our proposed method represents manifold-valued sequential data via practical computation based on well-defined mathematical formulations. In particular, we introduce a recurrent neural model on the Cholesky space by which it becomes possible to greatly enhance computational efficiency and to train network parameters with the conventional backpropagation. Moreover, the proposed method successfully learns real-world continuous data modeling using an RNN-based network with the help of manifold ODE for dynamics representation. To prove the robustness of our proposed method, we conducted experiments on two real-world tasks of video action recognition and sleep staging classification. Experimental results showed that our method learns powerful representations of data, achieving promising performances.

In summary, there are three major contributions of this work as follows:

- We devise a novel recurrent model that exploits a diffeo-

morphism mapping from SPD space to Cholesky space and operations corresponding to operations in Euclidean space.

- We develop a manifold ODE that represents temporal dynamics inherent in time-series data.
- We demonstrate the effectiveness of the proposed method through experiments for two real-world applications, achieving state-of-the-art performance, respectively.

The rest of this work is organized as follows: Section 2 briefly reviews related researches. In Section 3, we describe some important preliminary concepts for the proposed method. Then, Section 4 introduces the proposed method, which exploits an RNN-based architecture with the diffeomorphism estimation. Section 5 describes experimental settings in detail for reproducibility and results by comparing with competing methods in the literature. Finally, Section 6 concludes this study and suggests future research directions.

2 Related Work

Deep Learning on SPD Manifold. Recently manifold-valued data, especially SPD matrix, has been actively studied in deep neural models. In (Huang and Van Gool 2017), the author proposed SPDNet that consists of fully connected convolution-like layers, rectified linear units-like layers, and eigenvalue logarithm layers to train the deep model while maintaining the data structure on the SPD matrix. Subsequently, (Brooks et al. 2019) redefined the batch normalization on SPDNet using Riemannian operations for improving the classification performance as well as the robustness of the model. In (Suh and Kim 2021), the author proposed a metric learning-based SPD model that divides the classification problem with sub-problems and builds a single model to solve each sub-problem. Succinctly, SPDNet models are presented based on mapping with sub-manifold, but the repeating eigenvalue decomposition in this process inevitably generates tremendous computation cost.

Meanwhile, (Chakraborty et al. 2018) proposed a deep model based on statistical machine learning when data is ordered, longitudinal or temporal in Riemannian manifold. In addition, to solve the slow speed issue of RNN-based models, the dilated CNNs and causal CNNs were defined in the manifold space (Chakraborty et al. 2020; Zhen et al. 2019). In (Zhen et al. 2020), a flow-based generative model for manifold-valued data was introduced through three types of invertible layers in a generative regime. Basically, training a deep model while maintaining the SPD constraint is challenging because of huge computational costs and unstable training. In contrast, our proposed method can manage to address such limitations by means of diffeomorphism mapping into Cholesky space.

Neural ODEs. Foremost, (Chen et al. 2018) proposed the idea of parameterizing derivatives of hidden states for continuous modeling. Inspired by neural ODEs, (Rubanova, Chen, and Duvenaud 2019) proposed latent ODE and ODE-RNN to deal with irregularly-sampled data. Recent studies on the use of neural ODEs have begun modeling on structured (Xhonneux, Qu, and Tang 2020) or manifold-valued

data (Lou et al. 2020). In order to characterize the continuous of node representations, (Xhonneux, Qu, and Tang 2020) proposed a graph-based model. There are also recent studies on normalizing flow using neural ODEs in manifold space (Lou et al. 2020; Falorsi and Forré 2020). In light of this, our model also utilizes the neural ODEs in manifold space by focusing on continuous-time series modeling.

3 Preliminaries

In this section, we concisely provide useful definitions and operations for Riemannian geometry¹. It should be noted that our development is based on the diffeomorphism mapping of Cholesky decomposition, thus in Riemannian Cholesky space rather than in the Riemannian geometry of $n \times n$ symmetric positive definite matrices. In the following, $[\cdot]$ and $\mathcal{D}(\cdot)$ denote, respectively, the strictly lower triangular and the diagonal part of a matrix.

Riemannian Manifold and Metric on Cholesky Space

(Lin 2019). A Riemannian manifold (\mathcal{M}, g) is a real, smooth manifold \mathcal{M} equipped with a positive-definite inner product g_X on the tangent space $\mathcal{T}_X \mathcal{M}$ at each point $X \in \mathcal{M}$. The g_X is called a Riemannian metric, making it possible to define several geometric notions on a Riemannian manifold, such as angle and curve length.

The space \mathcal{S}_d^+ of $d \times d$ SPD matrices is a smooth submanifold of the space \mathcal{S}_d of symmetric matrices, whose tangent space at a given SPD matrix is identified with \mathcal{S}_d . Cholesky decomposition represents a matrix $S \in \mathcal{S}_d^+$ as a product of a lower triangular matrix L and its transpose, i.e., $S = LL^\top$. The smooth submanifold \mathcal{L}_+ of the space of lower triangular matrices \mathcal{L} with diagonal elements all positive defines a Cholesky space. Note that the tangent space of \mathcal{L}_+ at a given $L \in \mathcal{L}_+$ is identified with the linear space \mathcal{L} . Let the strict lower triangular space $[\mathcal{L}] = \{[X] | X \in \mathcal{L}\} \in \mathbb{R}^{d(d-1)/2}$ with the Frobenius inner product $\langle X, Y \rangle_F = \sum_{i,j=1}^d X_{ij}Y_{ij}$, $\forall X, Y \in [\mathcal{L}]$, while denoting the diagonal part $\mathcal{D}(\mathcal{L}) = \{\mathcal{D}(X) | X \in \mathcal{L}\}$ with a different inner product $\langle \mathcal{D}(L)^{-1}\mathcal{D}(X), \mathcal{D}(L)^{-1}\mathcal{D}(Y) \rangle_F$. Then, we define a metric \tilde{g} for tangent spaces $\mathcal{T}_L \mathcal{L}_+$ as follows:

$$\begin{aligned} \tilde{g}_L(X, Y) &= \langle X, Y \rangle_F + \langle \mathcal{D}(L)^{-1}\mathcal{D}(X), \mathcal{D}(L)^{-1}\mathcal{D}(Y) \rangle_F \\ &= \sum_{i>j} X_{ij}Y_{ij} + \sum_{j=1}^d X_{jj}Y_{jj}L_{jj}^{-2}. \end{aligned} \quad (1)$$

Proposition 1. *Cholesky map \mathfrak{L} is a diffeomorphism between smooth manifolds \mathcal{L}_+ and \mathcal{S}_d^+ .*

The full proof of Proposition 1 can be found in (Lin 2019).

Exponential and Logarithmic Map (Lin 2019) For any $P \in \mathcal{S}_d^+$ and $Q \in \mathcal{S}_d$, the exponential map $\text{Exp}_P : \mathcal{S}_d \rightarrow \mathcal{S}_d^+$ and the logarithmic map $\text{Log}_Q : \mathcal{S}_d^+ \rightarrow \mathcal{S}_d$ are defined as:

$$\text{Exp}_P(Q) = P^{\frac{1}{2}} \exp(P^{\frac{1}{2}} Q P^{-\frac{1}{2}}) P^{\frac{1}{2}} \in \mathcal{S}_d^+ \quad (2)$$

$$\text{Log}_Q(P) = Q^{\frac{1}{2}} \log(Q^{\frac{1}{2}} P Q^{-\frac{1}{2}}) Q^{\frac{1}{2}} \in \mathcal{S}_d \quad (3)$$

¹See Supplementary A to compare basic properties of Riemannian and Cholesky manifolds.

Generally, it is not easy to compute Riemannian exponential and logarithmic maps, because they require evaluating a series of an infinite number of terms. However, by mapping to Cholesky space, we can get easy-to-compute expressions for Riemannian exponential and logarithmic maps. Let $X \in \mathcal{L}_+$ and $K \in \mathcal{L}$. Then, we can define the exponential map $\widetilde{\text{Exp}}_X$ and the logarithmic map $\widetilde{\text{Log}}_K$ as:

$$\widetilde{\text{Exp}}_X(K) = \lfloor X \rfloor + \lfloor K \rfloor + \mathcal{D}(X) \exp\{\mathcal{D}(K)\mathcal{D}(X)^{-1}\} \quad (4)$$

$$\widetilde{\text{Log}}_K(X) = \lfloor X \rfloor - \lfloor K \rfloor + \mathcal{D}(K) \log\{\mathcal{D}(K)^{-1}\mathcal{D}(X)\}. \quad (5)$$

Fréchet Mean. The Fréchet mean (Fréchet 1948) is an extension of the Euclidean mean that is widely used to aggregate representations in neural networks such as attention (Vaswani et al. 2017) and batch normalization (Ioffe and Szegedy 2015), showing strong theoretical and practical interest in Riemannian data analysis. Given $\{P_i\}_{i=1}^N$ samples on \mathcal{M} , the Fréchet mean is defined as

$$\mu = \arg \min_{G \in \mathcal{S}_d^+} \sum_{i=1}^N d^2(G, P_i). \quad (6)$$

Unfortunately, the solution to the minimization problem is not known in closed-form, but usually computed using an iterative solver, *e.g.*, Karcher flow (Karcher 1977), that approximates the solution by computing in tangent space and mapping back to manifold space via logarithmic and exponential maps, respectively. However, the Fréchet mean in Cholesky space is closed and easy to compute. In other words, iterative operation is not required. We call this the *log-Cholesky* mean $\mu_{\mathcal{L}_+}$ and it is defined as (Lin 2019):

$$\mu_{\mathcal{L}_+} = \frac{1}{N} \sum_{i=1}^N \lfloor X_i \rfloor + \exp \left\{ N^{-1} \sum_{i=1}^N \log \mathcal{D}(X_i) \right\}. \quad (7)$$

Manifold ODE (Lou et al. 2020). We introduce the ordinary differential equation defined in manifold space. A manifold ODE defines a state $\mathbf{z} : [t_s, t_e] \rightarrow \mathcal{M}$ relating to vector field f in regard to the dynamics between two time points of t_s and t_e with an initial condition $z_s = \mathbf{z}(t_s)$:

$$\frac{d\mathbf{z}(t)}{dt} = f(\mathbf{z}(t), t) \in \mathcal{T}_{\mathbf{z}(t)}\mathcal{M}. \quad (8)$$

4 Continuous Manifold Learning on Riemannian Cholesky Space

In this section, we introduce the proposed continuous manifold learning method in Cholesky space for sequential manifold-valued data. The overall procedures are illustrated in Figure 1.

4.1 Mapping to Riemannian Cholesky Space

For manifold learning, we first need to map the input space into manifold space. Specifically, we exploit a second-order statistics (*i.e.*, covariance) of features, estimated by a shrinkage estimator (Chen et al. 2010), to represent an SPD matrix

in manifold space. Then, an SPD matrix S is decomposed into a lower triangular matrix X and its transpose X^\top by Cholesky decomposition $C(S) = XX^\top$. We express the lower triangular matrix X as the sum of the strictly lower part and the diagonal part as $X = \lfloor X \rfloor + \mathcal{D}(X)$.

In general, it is challenging to train a network in SPD Riemannian manifold because (1) there are various constraints in optimization, *e.g.*, convexity of weights in FM estimation (Chakraborty et al. 2018), validity of the output to be an SPD matrix (Huang and Van Gool 2017), and (2) numerical errors occur by the distortion of the geometrical structure during the learning process, especially when the dimension of a matrix increases (Dong et al. 2017). Meanwhile, due to the nice properties of Cholesky matrices, we only need to consider the constraint that the elements of the diagonal matrix $\mathcal{D}(X)$ should be positive, and the elements in $\lfloor X \rfloor$ are unconstrained. Thus, by taking advantage of operating in Cholesky space, it becomes relatively easy to solve an optimization problem.

4.2 Recurrent Network Model in Cholesky space

An RNN equipped with gated recurrent units (GRU) (Cho et al. 2014) has been successfully used for time-series modeling in various applications. Here, we introduce a novel Riemannian manifold GRU (RGRU) by reformulating gating operations in Cholesky space. Compared to the existing deep learning methods for SPD matrices modeling (Chakraborty et al. 2018; Zhen et al. 2020, 2019; Chakraborty et al. 2020; Huang and Van Gool 2017; Brooks et al. 2019; Gao et al. 2020; Suh and Kim 2021), as we formulate the optimization problem in Cholesky space with a unique constraint of positivity in values of the diagonal part of $\mathcal{D}(X)$, the optimization can be solved relatively easily along with efficient computations, thus making their computation costs cheap.

Let us reformulate the gating operations and feature representations in terms of Cholesky geometry with (i) weighted Fréchet mean (wFM), (ii) bias addition, and (iii) non-linearity. First, the wFM can be defined by using Eq. (7) for the weighted combination of Cholesky matrices as follows:

$$\begin{aligned} \text{wFM}(\{X_i\}_{i=1, \dots, N}, \mathbf{w} \in \mathcal{R}_{\geq 0}) \\ = \frac{1}{N} \sum_{i=1}^N (w_i \cdot \lfloor X_i \rfloor) \\ + \exp \left\{ N^{-1} \sum_{i=1}^N w_i \cdot \log \mathcal{D}(X_i) \right\}. \end{aligned} \quad (9)$$

where $\in \mathcal{R}_{\geq 0}$ denotes a space of non-negative real numbers and w_i denotes the i -th element of the weighted vector \mathbf{w} . Second, for the bias addition, we define an operator \oplus on \mathcal{L}_+ (Lin 2019) by

$$X \oplus Y = \lfloor X \rfloor + \lfloor Y \rfloor + \mathcal{D}(X)\mathcal{D}(Y). \quad (10)$$

\oplus is a smooth commutative group operation on the manifold \mathcal{L}_+ . Since this group operation is a bi-invariant metric, we regard operation for *translation*, analogous to the case in Euclidean space. Third, in regard to the non-linearity, since the off-diagonal values are unconstrained but the diagonal

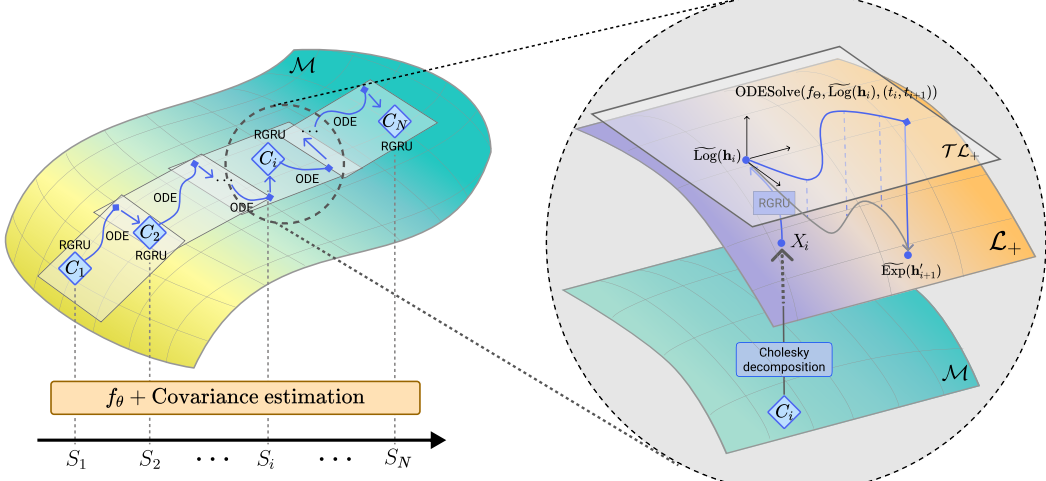


Figure 1: The overall framework of the proposed method. First, input sequence $\{S_i\}_{1, \dots, N}$ are fed into a feature extraction network f_θ for high-level representation. The manifold point $\{C_i\}_{1, \dots, N}$ obtained by covariance estimation is then decomposed to $\{X_i\}_{1, \dots, N}$ on Cholesky space. Riemannian manifold gated recurrent unit (RGRU) calculates Cholesky points, then the estimated points are mapped into the tangent space of the ordinary differential equation (ODE) solver, ODESolve through a logarithm map $\widetilde{\text{Log}}(\cdot)$. Afterwards, the output of the ODE solver at the i -th timepoint h'_i is projected to Cholesky space \mathcal{L}_+ by an exponential map, $\widetilde{\text{Exp}}(\cdot)$.

values should be positive, we handle elements of the off-diagonal part and the diagonal part separately by applying independent two activation functions accordingly and then add the resulting values to be a valid Cholesky matrix, *e.g.*, $X' = \tanh(\lfloor X \rfloor) + \text{softplus}(\mathcal{D}(X))$.

Given an input sequence $\mathbf{X} = \{\mathbf{x}_1, \mathbf{x}_2, \dots, \mathbf{x}_t\}$ on \mathcal{L}_+ , we reformulate the gating and representation operations involved in RGRU as follows:

$$\begin{cases} \mathbf{z}_i = \sigma(\mathbf{w}_{\text{FM}}(\{\mathbf{x}_i, \mathbf{h}_{i-1}\}, \mathbf{w}_z) \oplus \mathbf{b}_z) \\ \mathbf{r}_t = \sigma(\mathbf{w}_{\text{FM}}(\{\mathbf{x}_i, \mathbf{h}_{i-1}\}, \mathbf{w}_r) \oplus \mathbf{b}_r) \\ \mathbf{l}_i = \mathbf{w}_{\text{FM}}(\{\mathbf{x}_i, \mathbf{r}_i \odot \mathbf{h}_{i-1}\}, \mathbf{w}_l) \oplus \mathbf{b}_l \\ \hat{\mathbf{h}}_i = \tanh(\lfloor \mathbf{l}_i \rfloor) + \text{softplus}(\mathcal{D}(\mathbf{l}_i)) \\ \mathbf{h}_i = (1 - \mathbf{z}_i) \odot \mathbf{h}_{i-1} + \mathbf{z}_i \odot \hat{\mathbf{h}}_i \end{cases} \quad (11)$$

where $\mathbf{h}_i \in \mathcal{L}_+$ is the hidden state in RGRU, $\mathbf{z}_i \in \mathcal{L}_+$, $\mathbf{r}_i \in \mathcal{L}_+$ and $\hat{\mathbf{h}}_i \in \mathcal{L}_+$ are the update gate, the reset gate, and candidate hidden state, respectively; $\{\mathbf{w}_z \in \mathcal{L}_+, \mathbf{w}_r \in \mathcal{L}_+, \mathbf{w}_l \in \mathcal{L}_+\}$ are learnable weights and $\{\mathbf{b}_z \in \mathcal{L}_+, \mathbf{b}_r \in \mathcal{L}_+, \mathbf{b}_l \in \mathcal{L}_+\}$ are learnable biases; $\sigma(\cdot)$ is a logistic sigmoid function, $\tanh(\cdot)$ is a hyperbolic tangent function, and $\text{softplus}(\cdot)$ is a softplus function; and \odot denotes an operator of element-wise summation that works satisfying the group axiom. Since the values passed through the sigmoid function is always positive, it satisfies the constraint, but in the case of other activation functions such as hyperbolic tangent, a softplus function is further used for the diagonal part to guarantee the residence in Cholesky space. Without loss of generality, any activation function with a positive output range can be used in the position of a softplus function.

4.3 Neural Manifold ODEs

In order for continuous manifold learning, we further leverage the technique of neural manifold ODEs (Lou et al. 2020)

in sequential data modeling and model the dynamics of f in Eq. (8) by a neural network with its learnable parameters θ . Here, we define a forward pass and a backward pass gradient computation for network parameters learning. It should be noted that the forward pass is computed in manifold space but the backward pass is defined solely through an ODE in Euclidean space.

Forward Mode. Forward mode integration is broadly classified into two groups: a projection method (Hairer 2011) and an implicit method (Lou et al. 2020; Hairer 2011; Crouch and Grossman 1993). In this work, we employ an implicit method due to its general applicability in any manifold space and its definition using step-based solvers (Bielecki 2002; Crouch and Grossman 1993). In particular, we use a variant of an Euler method solver with an update step $h_{t+\epsilon} = \exp_{h_t}(\epsilon f(h_t, t))$ for the Riemannian exponential map (Bielecki 2002).

Backward Mode. Recently, (Chen et al. 2018) and (Lou et al. 2020) proposed an adjoint sensitivity method to effectively compute the gradients and to calculate the derivative of a manifold ODE, independently. In our method, we use their adjoint method to compute the derivative of a manifold ODE.

In differential geometry, $D_x f : \mathcal{T}_x \mathcal{M} \rightarrow \mathcal{T}_x \mathcal{N}$ defines a derivative of a function $f : \mathcal{M} \rightarrow \mathcal{N}$ mapping between two manifolds.

Theorem 1 (Lou et al. 2020). *We define some loss function $E : \mathcal{M} \rightarrow \mathbb{R}$. Suppose that there is an embedding of manifold space \mathcal{M} in Euclidean space \mathbb{R}^d . Let the adjoint*

Algorithm 1: ODE-RGRU

Input: Data point and their timestamps $\{(S_i, t_i)\}_{i=1,\dots,N}$
Output: $\{\mathbf{o}_i\}_{1,N}$

- 1: $S' = f_\theta(S)$
- 2: $C = \text{Shrinkage estimation}(S') \in \mathcal{S}_d^+$
- 3: $XX^\top = \text{Cholesky decomposition}(C)$
- 4: $\mathbf{h}_0 = \text{Identity matrix } I$
- 5: **for** i in $1, 2, \dots, N$ **do**
- 6: $\mathbf{h}'_i = \text{ODESolve}(f_\phi, \widetilde{\text{Log}}(\mathbf{h}_{i-1}), (t_{i-1}, t_i))$
- 7: $\mathbf{h}_i = \text{RGRU}(\widetilde{\text{Exp}}(\mathbf{h}'_i), X_i)$
- 8: **end for**
- 9: $\mathbf{o}_i = \text{OutputNN}(\mathbf{h}_i)$ for all $i = 1, \dots, N$
- 10: **return** $\{\mathbf{o}_i\}_{1,\dots,N}$

state be $\mathbf{a}(t) = D_{\mathbf{z}(t)}E$, then the adjoint satisfies

$$\frac{d\mathbf{a}(t)}{dt} = -\mathbf{a}(t)D_{\mathbf{z}}(t)f(\mathbf{z}(t), t) \quad (12)$$

Refer to (Lou et al. 2020) for full proof. With the adjoint state, we calculate the gradients with respect to the start and the end time points, t_s, t_e , the initial condition \mathbf{z}_s , and the weights in Eq. (8).

4.4 ODE-RGRU

Now, we describe to combine manifold ODE and RGRU in a unified framework for sequential continuous manifold modeling, called ODE-RGRU. Formally, the ODE-RGRU is formulated as

$$\mathbf{h}'_i = \text{ODESolve}(f_\Theta, \widetilde{\text{Log}}(\mathbf{h}_{i-1}), (t_{i-1}, t_i)) \quad (13)$$

$$\mathbf{h}_i = \text{RGRU}(\widetilde{\text{Exp}}(\mathbf{h}'_i), X_i), \quad (14)$$

where $X_i \in \mathcal{L}_+$ is an input feature and \mathbf{h}_i is a latent state at the i -th timepoint, for $i = 1, \dots, N$. We define a hidden state \mathbf{h}_i to be the solution on tangent space to an ODESolver and then the output of ODESolver is orthogonally projected to manifold space by an exponential map. For each observation over time, the corresponding hidden state is updated using RGRU in Cholesky space by using Eq. (11). The overall algorithm is given in Algorithm 1.

4.5 Computational Time Efficiency

To learn geometric information in a neural network through manifold learning, the internal operations should consider and satisfy manifold constraints. In particular, the SPD matrix appears in various domains, but it is difficult to train a neural network because of hard constraints (symmetries and all positive eigenvalues). To tackle such challenges, (Huang and Van Gool 2017) trained their model in a compact Stiefel manifold space and (Gao et al. 2020) applied Euclidean operations in a tangent space with a logarithmic map and switched to manifold space with an exponential map. Most operations are performed through the Eigenvalue decomposition with a computational complexity of $O(k \cdot n^3)$ on k iterations. That is, as the dimension of matrices of interest increases, the computational cost increases dramatically. In

this regard, it was involved to map into a smaller dimension first so that manifold learning could be performed in a reasonable computational time. However, it still remains that no closed-form solution exists for the Fréchet mean, thus making the model training unstable.

In this work, we propose to exploit the Cholesky decomposition, which finds a unique lower triangular matrix for an SPD matrix. The nice properties of a Cholesky matrix allow efficient numerical calculations. And it has simple and easy-to-compute expressions for Riemannian exponential and logarithmic maps. Notably, it provides a closed-form solution for the Fréchet mean with a linear computational complexity.

5 Experiments

In this section, we evaluate the proposed method for two real-world applications of video action recognition and sleep staging classification by using public datasets. Our code is available at <https://github.com/Jeongseungwoo/Efficient-Continuous-Manifold-Learning>.

5.1 Datasets and Preprocessing

Action Recognition. For the action recognition task, we used UCF11 (Liu, Luo, and Shah 2009) dataset. The UCF11 dataset is composed of 1,600 video clips in total, containing 11 action categories, *e.g.*, basketball shooting, biking/cycling, diving, golf swinging, etc. The length of video frames varies from 204 to 1492 per clip with a resolution of each frame being 320×240 . Similar to the previous work of (Zhen et al. 2019; Chakraborty et al. 2018), we downsized all frames to 160×120 and sampled 50 frames from each clip, *i.e.*, $N = 50$, with an equal time gap between frames. Then, we performed the 5-fold cross-validation for fair evaluation while keeping the class-balance.

Sleep Staging Classification. We used SleepEDF-20 (Goldberger et al. 2000) dataset for the sleep staging classification task. The SleepEDF-20 is the Sleep Cassette that comprised of 20 subjects (10 males and 10 females) aged 25-34. Two polysomnographies were recorded during day-night periods except for subject 13 who had lost the second night due to a device problem. All signals were segmented with a length of 30 seconds and manually labeled into 8 categories, ‘wake,’ ‘rapid eye movement (REM),’ ‘non REM1/2/3/4,’ ‘movement,’ and ‘unknown,’ by sleep experts (Rechtschaffen 1968). In this work, similar to the previous studies in (Phan et al. 2018a,c; Supratak et al. 2017; Phan et al. 2021), we merged ‘non REM3’ and ‘non REM4’ stages into ‘non REM3’ stage and removed samples labeled as ‘movement’ and ‘unknown.’ Here, we used spectrogram data rather than raw signals. To do so, we sampled all signals at 100Hz rate and applied short-time Fourier transformation to compute spectrograms. For this experiment, we used single-channel electroencephalogram (EEG) and 2-channels EEG/electrooculogram (EOG) samples. Note that we did not exploit electromyogram recordings due to its incompleteness. As a result, we obtained a multi-channel signal $S \in \mathbb{R}^{F \times T \times C}$ where F , T , and C denote the number of frequency bins, the number of spectral columns, and the num-

ber of channels, respectively. We set $F = 129$, $T = 29$, $C = 1$ or $C = 2$ (for the single-channel EEG or two-channels EEG/EOG). For the staging classification, continuous 10 segments of data were used as input, *i.e.*, $N = 10$. For fair evaluation, we conducted the 20-fold cross-validation by maintaining the class-balance same as (Phan et al. 2018a,c; Supratak et al. 2017; Phan et al. 2021).

5.2 Experimental Settings

Action Recognition. In our work, we compared the proposed method with state-of-the-art manifold learning methods as well as traditional deep learning models in the action recognition task. For the baseline methods that represent data in Euclidean space, we exploited GRU (Cho et al. 2014), long short-term memory (LSTM) (Hochreiter and Schmidhuber 1997), TT-GRU, and TT-LSTM (Yang, Krompass, and Tresp 2017). For GRU and LSTM, we first extracted spatial features using 3 convolutional layers with a kernel size of 7×7 and channel dimensions of 10, 15, and 25, respectively. Further, batch normalization (Ioffe and Szegedy 2015), leaky rectified linear units (LeakyReLU) (Maas et al. 2013), and max pooling were followed after each convolutional layer. Then, the extracted spatial features were flattened and fed into the recurrent models, *i.e.*, GRU and LSTM, both of which had 50 hidden nodes. For TT-GRU and TT-LSTM, we reshaped an input sample to $8 \times 20 \times 20 \times 18$ and set the rank size to $1 \times 4 \times 4 \times 4 \times 1$. Finally, we obtained a $4 \times 4 \times 4 \times 4$ output.

For the other baseline methods considered in the action recognition experiments, we employed SPDSRU (Chakraborty et al. 2018) and ManifoldDCNN (Zhen et al. 2019). For covariance matrices used in SPDSRU and ManifoldDCNN, we adopted a covariance block analogous to (Yu and Salzmann 2017) to get the reported testing accuracies. Then, for SPDSRU, 2 convolutional layers with 7×7 kernels, 7 channels for the final output were chosen, therefore the dimension of the covariance matrices was 8×8 same as (Chakraborty et al. 2018). Finally, based on (Zhen et al. 2019), ManifoldDCNN also used 2 convolutional layers with 7×7 kernels and set 6 channels for the final output, *i.e.*, the dimension covariance matrices was 7×7 .

While training our proposed method, we chose 3 convolutional layers with a kernel size of 7×7 and exploited batch normalization (Ioffe and Szegedy 2015), LeakyReLU activation (Maas et al. 2013), and max pooling for f_θ . Further, we set the number of output dimension to 32, *i.e.*, the dimension of SPD matrix was 32×32 . In this respect, the diagonal matrix and strictly lower triangular matrix obtained through Cholesky decomposition was expressed as a 32-dimensional vector and a vector of $32 \times (32 - 1)/2$ in dimension, respectively. Moreover, similar to neural ODEs (Chen et al. 2018), we employed a multilayer perceptron (MLP) with a tanh activation for f_ϕ . Finally, we set the number of hidden units 100 for RGRU.

Sleep Staging Classification. For the sleep staging classification experiments, we compared our proposed method with the state-of-the-art methods of XSleepNet (Phan et al. 2021), SeqSleepNet (Phan et al. 2019), FCNN+RNN (Phan

Table 1: Performance (mean \pm std, %) on an action recognition task (UCF11).

Method	# Parameters	Accuracy
Proposed ODE-RGRU	66,767	89.4 ± 1.2
ManifoldDCNN (Zhen et al. 2019)	3,658	82.3 ± 1.8
SPDSRU (Chakraborty et al. 2018)	3,445	78.4 ± 1.4
TT-GRU (Yang, Krompass, and Tresp 2017)	202,667	81.3 ± 1.1
TT-LSTM (Yang, Krompass, and Tresp 2017)	6,176	79.6 ± 3.5
GRU	18,602,606	79.3 ± 3.8
LSTM	24,791,606	71.4 ± 2.7

et al. 2021), DeepSleepNet (Supratak et al. 2017), U-time (Perslev et al. 2019), and IITNet (Seo et al. 2020). We reported the performance of those competing methods by taking from (Phan et al. 2021).

By following (Phan et al. 2021), we used a filterbank layer (Phan et al. 2018b) for time-frequency input data. Through the learnable filterbank layer, the spectral dimension of the input data was reduced from $F = 129$ to 32. Here, 2 convolutional layers followed by batch normalization and a LeakyReLU activation were used for f_θ . The output dimension was set as 8, *i.e.*, the dimension of SPD matrix was 8×8 . Then, we also used an MLP with a tanh for f_ϕ and set 50 hidden units for RGRU. Finally, since sleep staging of a sample is related to neighboring samples, we also exploited a bidirectional structure in RGRU to take into account such useful information, same as other competing methods.

Additional Implementation Details. For both action recognition and sleep staging classification experiments, we used a multi-class cross-entropy loss and employed an Adam optimizer with a learning rate of 10^{-4} and an ℓ^2 regularizer with its weighting coefficient of 10^{-3} . We trained our proposed network for 1,000 (for the action recognition) or 20 (for the sleep staging classification) epochs with a batch size of 32. For the learnable parameters of RGRU, which should be in Cholesky space, *i.e.*, $\mathbf{w}_z, \mathbf{w}_r, \mathbf{w}_l, \mathbf{b}_z, \mathbf{b}_r, \mathbf{b}_l \in \mathcal{L}_+$, we only needed to care about the diagonal elements. In order for that, we simply applied an absolute operator during backpropagation²

5.3 Experimental Results

Action Recognition. As presented in Table 1, the proposed method outperformed the competing baseline methods with large margin (7.1% \sim 18.0%). Notably, the proposed method achieved the best performance although the number of its tunable parameters was significantly smaller than the other Euclidean representation-based methods. Based on these promising results, we believe that the pro-

²See Supplementary B for detailed model architectures used in the action recognition and the sleep staging classification experiments.

Table 2: Performance on sleep staging classification task (SleepEDF-20). We computed accuracy (Acc), Cohen’s kappa value (κ), macro F1-score (MF1), averaged sensitivity (Sens), and averaged specificity (Spec).

Method	EEG					EEG/EOG				
	Acc	κ	MF1	Sens	Spec	Acc	κ	MF1	Sens	Spec
Proposed ODE-RGRU	86.3	0.807	80.2	80.6	96.3	86.6	0.812	80.3	81.4	96.4
XSleepNet (Phan et al. 2021)	86.3	0.813	80.6	80.2	96.4	86.4	0.813	80.9	79.9	96.2
SeqSleepNet (Phan et al. 2019)	85.2	0.798	78.4	78.0	96.1	86.0	0.809	79.7	79.2	96.2
FCNN + RNN (Phan et al. 2021)	81.8	0.754	75.6	75.7	95.3	83.5	0.775	77.7	77.2	95.5
DeepSleepNet (Supratak et al. 2017)	-	-	-	-	-	82.0	0.760	76.9	-	-
U-time (Perslev et al. 2019)	-	-	79.0	-	-	-	-	-	-	-
IITNet (Seo et al. 2020)	83.9	0.780	77.6	-	-	-	-	-	-	-

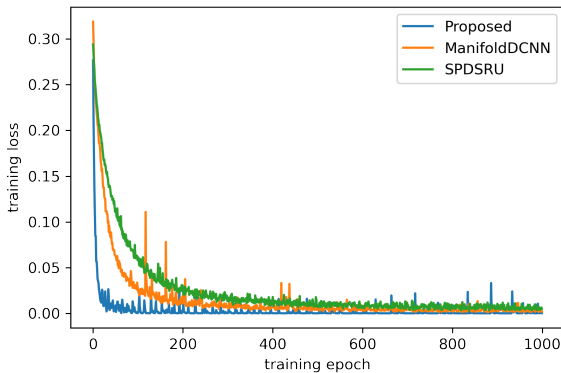


Figure 2: Training loss curve of the manifold methods for the UCF11 dataset.

posed method could learn geometric features in complex actions efficiently.

Sleep Staging Classification. For the sleep staging classification task, we evaluated accuracy (Acc), Cohen’s kappa value (κ) (McHugh 2012), macro F1-score (MF1) (Yang and Liu 1999), averaged sensitivity (Sens), and averaged specificity (Spec) and reported in Table 2. In the single-channel EEG experiment, our proposed method showed an accuracy of 86.3% and a sensitivity of 80.6%, which were the same or higher than the comparative methods. Here, the proposed method achieved the accuracy of 86.3% and the sensitivity of 80.6%, the same or the highest score compared to competing baselines. Although XSleepNet (Phan et al. 2021) achieved slightly higher performance for the Cohen’s kappa value, the macro F1-score, and the specificity, the proposed method also showed comparable and plausible performance. Furthermore, it is worth noting that XSleepNet used both raw signals and spectrograms for its decision-making. For the two-channels EEG/EOG case, the proposed method outperformed all baseline methods for metrics of the accuracy, the sensitivity, and the specificity. On the other hand, our method also slightly underperformed than XSleepNet, which exploited complement data types.

Training Speed Our method uses Cholesky decomposition to map the SPD manifolds into Cholesky space. The Cholesky decomposition greatly reduces the computational costs, thereby allowing to use the larger SPD matrix than existing geometric deep learning methods (Huang and Van Gool 2017; Brooks et al. 2019). Therefore, by using the large SPD matrix, the proposed method could learn various features of the large dimensional input data. We compared the learning curves of three comparative manifold deep-learning methods in Figure 2. Remarkably, our proposed method showed its convergence faster and more stable than the others.

6 Conclusions

Manifold learning, especially training deep neural networks in SPD manifold, is challenging due to the constraints in an SPD matrix. In this paper, we proposed a novel continuous manifold neural network, called ODE-RGRU, by systematically combining GRU and ODE in Cholesky space, and efficiently resolving difficulties related to computational costs in optimization. Specifically, we first reformulated the gating operations in GRU, thus making it works in Riemannian manifold. Furthermore, in order to learn continuous geometric feature representations from sequential SPD-valued data, we additionally devised and applied a manifold ODE to the recurrent model. In our experiments on two tasks of video action recognition on the UCF11 dataset and sleep staging classification on the SleepEDF-20 dataset, we empirically demonstrated its effectiveness and suitability for time series modeling, by achieving state-of-the-art performance for both tasks.

Acknowledgements

This work was supported by Institute of Information & communications Technology Planning & Evaluation (IITP) grant funded by the Korea government (MSIT) (No. 2019-0-00079, Department of Artificial Intelligence (Korea University)) and by the Institute of Information & Communications Technology Planning & Evaluation (IITP) grant funded by the Korea government (No. 2017-0-00451; Development of BCI based Brain and Cognitive Computing Technology for Recognizing User’s Intentions using Deep Learning).

References

Bielecki, A. 2002. Estimation of the Euler method error on a Riemannian manifold. *Communications in numerical methods in engineering*, 18(11): 757–763.

Bronstein, M. M.; Bruna, J.; LeCun, Y.; Szlam, A.; and Vandergheynst, P. 2017. Geometric deep learning: going beyond euclidean data. *IEEE Signal Processing Magazine*, 34(4): 18–42.

Brooks, D.; Schwander, O.; Barbaresco, F.; Schneider, J.-Y.; and Cord, M. 2019. Riemannian batch normalization for SPD neural networks. In *Thirty-third Annual Conference on Neural Information Processing Systems*.

Brouwer, E. D.; Simm, J.; Arany, A.; and Moreau, Y. 2019. GRU-ODE-Bayes: continuous modeling of sporadically-observed time series. In *Proceedings of the 33rd International Conference on Neural Information Processing Systems*, 7379–7390.

Chakraborty, R.; Bouza, J.; Manton, J.; and Vemuri, B. C. 2020. Manifoldnet: A deep neural network for manifold-valued data with applications. *IEEE Transactions on Pattern Analysis and Machine Intelligence*.

Chakraborty, R.; Yang, C.; Zhen, X.; Banerjee, M.; Archer, D.; Vaillancourt, D.; Singh, V.; and Vemuri, B. 2018. A Statistical Recurrent Model on the Manifold of Symmetric Positive Definite Matrices. *Advances in neural information processing systems*.

Chang, A. X.; Funkhouser, T.; Guibas, L.; Hanrahan, P.; Huang, Q.; Li, Z.; Savarese, S.; Savva, M.; Song, S.; Su, H.; et al. 2015. Shapenet: An information-rich 3d model repository. *arXiv preprint arXiv:1512.03012*.

Chen, R. T.; Rubanova, Y.; Bettencourt, J.; and Duvenaud, D. 2018. Neural ordinary differential equations. In *Proceedings of the 32nd International Conference on Neural Information Processing Systems*, 6572–6583.

Chen, Y.; Wiesel, A.; Eldar, Y. C.; and Hero, A. O. 2010. Shrinkage algorithms for MMSE covariance estimation. *IEEE Transactions on Signal Processing*, 58(10): 5016–5029.

Cho, K.; Van Merriënboer, B.; Gulcehre, C.; Bahdanau, D.; Bougares, F.; Schwenk, H.; and Bengio, Y. 2014. Learning phrase representations using RNN encoder-decoder for statistical machine translation. *arXiv preprint arXiv:1406.1078*.

Crouch, P. E.; and Grossman, R. 1993. Numerical integration of ordinary differential equations on manifolds. *Journal of Nonlinear Science*, 3(1): 1–33.

Dong, Z.; Jia, S.; Zhang, C.; Pei, M.; and Wu, Y. 2017. Deep manifold learning of symmetric positive definite matrices with application to face recognition. In *Thirty-First AAAI Conference on Artificial Intelligence*.

Falorsi, L.; and Forré, P. 2020. Neural ordinary differential equations on manifolds. *arXiv preprint arXiv:2006.06663*.

Fréchet, M. 1948. Les éléments aléatoires de nature quelconque dans un espace distancié. In *Annales de l'institut Henri Poincaré*, volume 10, 215–310.

Gao, Z.; Wu, Y.; Jia, Y.; and Harandi, M. 2020. Learning to Optimize on SPD Manifolds. In *Proceedings of the IEEE/CVF Conference on Computer Vision and Pattern Recognition*, 7700–7709.

Goldberger, A. L.; Amaral, L. A.; Glass, L.; Hausdorff, J. M.; Ivanov, P. C.; Mark, R. G.; Mietus, J. E.; Moody, G. B.; Peng, C.-K.; and Stanley, H. E. 2000. PhysioBank, PhysioToolkit, and PhysioNet: components of a new research resource for complex physiologic signals. *circulation*, 101(23): e215–e220.

Hairer, E. 2011. Solving ordinary differential equations on manifolds. In *Lecture notes, University of Geneva*.

Hochreiter, S.; and Schmidhuber, J. 1997. Long short-term memory. *Neural computation*, 9(8): 1735–1780.

Huang, Z.; and Van Gool, L. 2017. A riemannian network for spd matrix learning. In *Proceedings of the AAAI Conference on Artificial Intelligence*, volume 31.

Ioffe, S.; and Szegedy, C. 2015. Batch normalization: Accelerating deep network training by reducing internal covariate shift. In *International conference on machine learning*, 448–456. PMLR.

Jayasumana, S.; Hartley, R.; Salzmann, M.; Li, H.; and Harandi, M. 2013. Kernel methods on the Riemannian manifold of symmetric positive definite matrices. In *Proceedings of the IEEE conference on computer vision and pattern recognition*, 73–80.

Karcher, H. 1977. Riemannian center of mass and mollifier smoothing. *Communications on pure and applied mathematics*, 30(5): 509–541.

Kendall, A.; and Cipolla, R. 2017. Geometric loss functions for camera pose regression with deep learning. In *Proceedings of the IEEE conference on computer vision and pattern recognition*, 5974–5983.

Kipf, T. N.; and Welling, M. 2016. Semi-supervised classification with graph convolutional networks. *arXiv preprint arXiv:1609.02907*.

Lin, Z. 2019. Riemannian geometry of symmetric positive definite matrices via cholesky decomposition. *SIAM Journal on Matrix Analysis and Applications*, 40(4): 1353–1370.

Liu, J.; Luo, J.; and Shah, M. 2009. Recognizing realistic actions from videos “in the wild”. In *2009 IEEE Conference on Computer Vision and Pattern Recognition*, 1996–2003. IEEE.

Lou, A.; Lim, D.; Katsman, I.; Huang, L.; Jiang, Q.; Lim, S.-N.; and De Sa, C. 2020. Neural manifold ordinary differential equations. *arXiv preprint arXiv:2006.10254*.

Maas, A. L.; Hannun, A. Y.; Ng, A. Y.; et al. 2013. Rectifier nonlinearities improve neural network acoustic models. In *Proc. icml*, volume 30, 3. Citeseer.

McHugh, M. L. 2012. Interrater reliability: the kappa statistic. *Biochimia medica*, 22(3): 276–282.

Moakher, M. 2005. A differential geometric approach to the geometric mean of symmetric positive-definite matrices. *SIAM Journal on Matrix Analysis and Applications*, 26(3): 735–747.

Perslev, M.; Jensen, M.; Darkner, S.; Jønnum, P. J.; and Igel, C. 2019. U-Time: A Fully Convolutional Network for Time Series Segmentation Applied to Sleep Staging. *Advances in Neural Information Processing Systems*, 32: 4415–4426.

Phan, H.; Andreotti, F.; Cooray, N.; Chén, O. Y.; and De Vos, M. 2018a. Automatic sleep stage classification using single-channel eeg: Learning sequential features with attention-based recurrent neural networks. In *2018 40th annual international conference of the IEEE engineering in medicine and biology society (EMBC)*, 1452–1455. IEEE.

Phan, H.; Andreotti, F.; Cooray, N.; Chén, O. Y.; and De Vos, M. 2018b. DNN filter bank improves 1-max pooling CNN for single-channel EEG automatic sleep stage classification. In *2018 40th annual international conference of the IEEE engineering in medicine and biology society (EMBC)*, 453–456. IEEE.

Phan, H.; Andreotti, F.; Cooray, N.; Chén, O. Y.; and De Vos, M. 2018c. Joint classification and prediction CNN framework for automatic sleep stage classification. *IEEE Transactions on Biomedical Engineering*, 66(5): 1285–1296.

Phan, H.; Andreotti, F.; Cooray, N.; Chén, O. Y.; and De Vos, M. 2019. SeqSleepNet: end-to-end hierarchical recurrent neural network for sequence-to-sequence automatic sleep staging. *IEEE Transactions on Neural Systems and Rehabilitation Engineering*, 27(3): 400–410.

Phan, H.; Chén, O. Y.; Tran, M. C.; Koch, P.; Mertins, A.; and De Vos, M. 2021. XSleepNet: Multi-view sequential model for automatic sleep staging. *IEEE Transactions on Pattern Analysis and Machine Intelligence*.

Rechtschaffen, A. 1968. A manual for standardized terminology, techniques and scoring system for sleep stages in human subjects. *Brain information service*.

Rezende, D.; and Mohamed, S. 2015. Variational inference with normalizing flows. In *International conference on machine learning*, 1530–1538. PMLR.

Rubanova, Y.; Chen, R. T.; and Duvenaud, D. K. 2019. Latent Ordinary Differential Equations for Irregularly-Sampled Time Series. *Advances in Neural Information Processing Systems*, 32: 5320–5330.

Scarselli, F.; Gori, M.; Tsoi, A. C.; Hagenbuchner, M.; and Monfardini, G. 2008. The graph neural network model. *IEEE transactions on neural networks*, 20(1): 61–80.

Seo, H.; Back, S.; Lee, S.; Park, D.; Kim, T.; and Lee, K. 2020. Intra-and inter-epoch temporal context network (IIT-Net) using sub-epoch features for automatic sleep scoring on raw single-channel EEG. *Biomedical Signal Processing and Control*, 61: 102037.

Suh, Y.-J.; and Kim, B. H. 2021. Riemannian embedding banks for common spatial patterns with eeg-based spd neural networks. In *Proceedings of the AAAI Conference on Artificial Intelligence (AAAI)*.

Supratak, A.; Dong, H.; Wu, C.; and Guo, Y. 2017. Deep-SleepNet: A model for automatic sleep stage scoring based on raw single-channel EEG. *IEEE Transactions on Neural Systems and Rehabilitation Engineering*, 25(11): 1998–2008.

Vaswani, A.; Shazeer, N.; Parmar, N.; Uszkoreit, J.; Jones, L.; Gomez, A. N.; Kaiser, Ł.; and Polosukhin, I. 2017. Attention is all you need. In *Advances in neural information processing systems*, 5998–6008.

Xhonneux, L.-P.; Qu, M.; and Tang, J. 2020. Continuous graph neural networks. In *International Conference on Machine Learning*, 10432–10441. PMLR.

Yang, Y.; Krompass, D.; and Tresp, V. 2017. Tensor-train recurrent neural networks for video classification. In *International Conference on Machine Learning*, 3891–3900. PMLR.

Yang, Y.; and Liu, X. 1999. A re-examination of text categorization methods. In *Proceedings of the 22nd annual international ACM SIGIR conference on Research and development in information retrieval*, 42–49.

Yu, K.; and Salzmann, M. 2017. Second-order convolutional neural networks. *arXiv preprint arXiv:1703.06817*.

Zhen, X.; Chakraborty, R.; Vogt, N.; Bendlin, B. B.; and Singh, V. 2019. Dilated convolutional neural networks for sequential manifold-valued data. In *Proceedings of the IEEE/CVF International Conference on Computer Vision*, 10621–10631.

Zhen, X.; Chakraborty, R.; Yang, L.; and Singh, V. 2020. Flow-based Generative Models for Learning Manifold to Manifold Mappings. *arXiv preprint arXiv:2012.10013*.